

Ground state terahertz quantum cascade lasers

Chun Wang I. Chan,^{1,a)} Qing Hu,¹ and John L. Reno²

¹*Department of Electrical Engineering and Computer Science, Massachusetts Institute of Technology, Cambridge, Massachusetts 02139, USA*

²*Center for Integrated Nanotechnologies, Sandia National Laboratories, MS 1303, Albuquerque, New Mexico 87185-1303, USA*

(Received 24 July 2012; accepted 1 October 2012; published online 9 October 2012)

A terahertz quantum cascade laser (THz QCL) architecture is presented in which only the ground state subbands of each quantum well are involved in the transport and lasing transition. Compared to state-of-the-art THz QCLs based on the resonant-phonon scheme, ground state QCLs employ narrower wells so that all high-energy subbands are pushed up far above the occupied subband levels, significantly reducing parasitic interactions. Data on the experimental realization of two types of ground state QCLs are presented, in which the result of lasing above 5 THz is demonstrated. © 2012 American Institute of Physics. [<http://dx.doi.org/10.1063/1.4759043>]

The adoption of terahertz quantum cascade lasers (THz QCLs) for practical applications is hindered by their need for cryogenic cooling, hence increasing THz QCL operation temperature remains the most important research goal in the field.¹ Although a conventional resonant-phonon (RP) structure has recently achieved $T_{\max} \sim 200$ K,² further improvements may require the exploration of unconventional laser designs. To this end, here we present preliminary results on ground state (GS) THz QCL designs, which employ no quantum-well excited states.

Parasitic subband interactions with high energy subbands are a suspected cause of temperature degradation in THz QCLs.³ Some theoretical results even suggest that such interactions may lead to electron transport that do not adhere to superlattice periodicity.⁴ GS QCLs seek to render these interactions energetically unfavorable by employing sufficiently narrow quantum wells such that all excited subbands are pushed high up into the conduction band. This simplifies the avoidance of high energy parasitics at the cost of a reduction in the selectivity of electron extraction from the lower lasing level. The loss of selectivity is because that depopulation occurs solely through longitudinal optical (LO)-phonon scattering without the assistance of resonant tunneling to enhance selectivity.

This ground state concept is not new.⁵ In fact, because of its simplicity, the first THz emitting structure based on LO-phonon scattering for depopulation employed this scheme, but lasing has never been experimentally realized.⁶ Here we present experimental results from two types of GS QCLs grown in the GaAs/Al_{0.30}Ga_{0.70}As material system. The band diagram of one such laser design, named OWIGS271, is shown in Fig. 1(a). This design is qualitatively the same as the one reported in Ref. 6. Even though it has the same number of wells (3) as the 3-well RP designs,^{2,7,8} there is a qualitative difference. The RP design has two subband levels in the phonon well (widest well) involved in electron transport, with the upper subband aligned with the lower lasing level at the designed bias. Because the two subbands in the phonon well are separated

by the LO phonon energy (~ 36 meV in GaAs), the width of this well tends to be much wider than other wells, resulting in parasitic subband levels not much higher in energy than the lasing levels. For example, in the 200 K design, the closest parasitic subband is 39 meV away from the upper laser level, whereas it is 57 meV away in OWIGS271. This greater energy barrier should strongly suppress undesired interactions in the latter.

There are several necessary trade-offs in the design. The lack of resonant tunneling in extraction reduces the selectivity of the extraction process. Thus, if the lower level lifetime is kept short (< 1 ps) by using a thin barrier, then the upper level lifetime can be preserved only by spatially separating the upper and lower lasing subbands; in other words, the radiative transition must be highly diagonal in space (the radiative oscillator strength normalized to the effective mass of GaAs for OWIGS271 is $f_{32} = 0.20$). Accounting only for LO phonon scattering, the calculated upper and lower levels lifetimes at high temperatures are 1.07 ps and 0.58 ps. While this depopulation is slow compared to the lifetime of the intrawell LO phonon emission commonly employed in RP THz QCLs, the overall degradation of effective extraction time from the lower lasing subband is mitigated somewhat by the lack of resonant tunneling for depopulation.⁹

OWIGS271 (wafer number VA0323) was grown by molecular beam epitaxy (MBE) with 271 cascaded modules, with $n = 5 \times 10^{18} \text{ cm}^{-3}$ Si doped contact layers grown above (50 nm) and below (100 nm) the $8 \mu\text{m}$ thick active region and a 200 nm Al_{0.55}Ga_{0.45}As etch-stop layer underlying the entire growth (the 100 nm contact layer is later removed by wet-etching). Laser ridges were clad in Ta/Cu metal-metal waveguides and patterned through wet-etching in 1:1:25 H₃PO₄: H₂O₂: H₂O. The fabricated devices were cleaved, indium soldered ridge side up on a copper mount, wire-bonded and mounted on the cold stage of a pulsed-tube cryocooler. Experimental data are shown in Fig. 2, in which lasing at ~ 5.2 THz is observed up to a heat sink temperature of 71 K.

Although OWIGS271 has identical bulk doping to published RP designs, its maximum current density is much lower. This is due to the extremely diagonal optical transition, which leads to the upper level lifetime being the

^{a)}Electronic mail: icwchan@mit.edu.

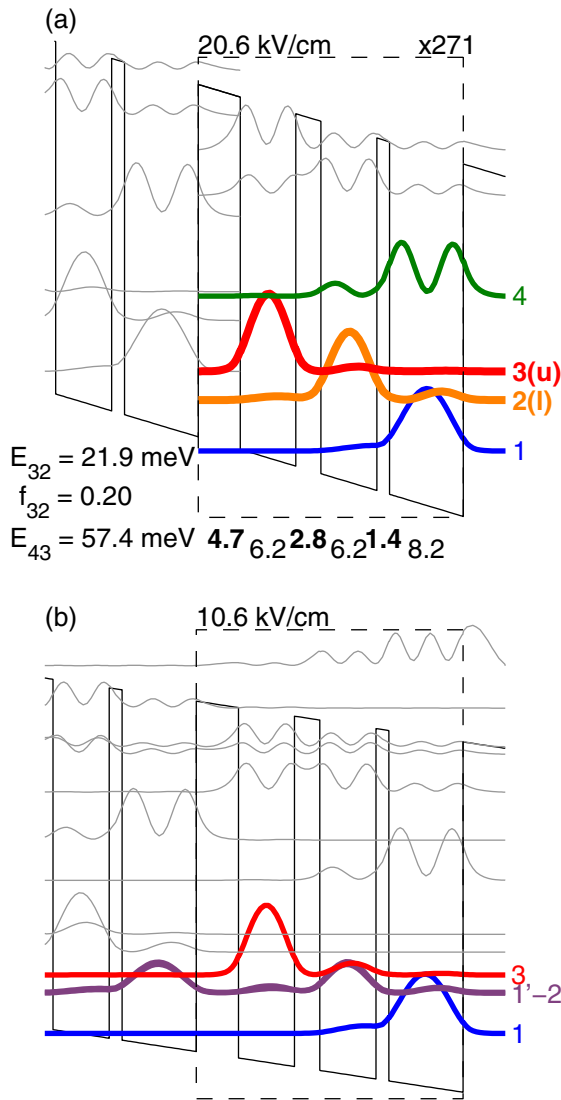


FIG. 1. (a) One module band diagram for OWIGS271. Layers are marked by their thicknesses in nm. The 8.2 nm well is doped to $2.4 \times 10^{16} \text{ cm}^{-3}$. (b) Two module band diagram for OWIGS271, showing parasitic interaction between injector and lower laser level ($1' - 2$).

bottleneck to transport. We may quantify this by comparing the Kazarinov-Suris tunneling time $\tau_{\text{tun}} = 1/2\Omega^2\tau_{\parallel}$ to the upper level lifetime, where $\Omega \approx \Delta/2\hbar$ is the tunnel coupling and τ_{\parallel} is the dephasing time. Using a calculated injection anticrossing of $\Delta = 2.02 \text{ meV}$ and estimating the dephasing time to be $\sim 0.33 \text{ ps}$, a tunneling time of $\sim 0.7 \text{ ps}$ is estimated. In comparison, the upper level lifetime assuming an electron temperature 80 K above lattice temperature is 6.0 ps. A more complete treatment using the rates equations approach of Ref. 10 yields $J_{\text{max}} \approx 450 \text{ A/cm}^2$ at 71 K, which is in reasonably good agreement with experiment. Similarly low current densities are observed in extremely diagonal three-well RP designs (see OWI210H in Ref. 11).

Examination of the $I-V$ characteristics reveals that OWIGS271 also shows a pronounced shoulder feature at biases below the onset of lasing operation, which is likely due to the resonant interaction of the injector subband with the lower lasing level in the next QCL period (see Fig. 2(b)).

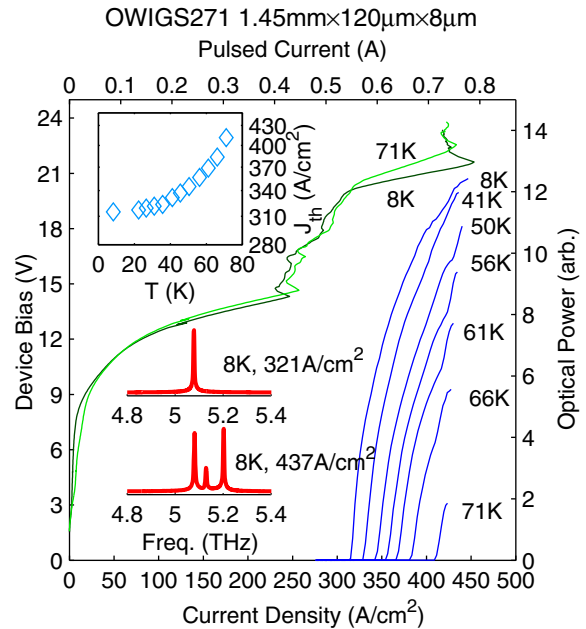


FIG. 2. Experimental data for OWIGS271 clad in Ta/Cu waveguides with wet-etched defined mesas.

This is a well known issue in one-well injector RP designs. In order to reduce this coupling between the injector and lower lasing levels, we attempt to suppress this parasitic in a second GS design, TWIGS254, by employing a two-well injector. The band diagram of TWIGS254 is shown in Fig. 3. The upper and lower level lifetimes are 1.07 ps and 0.45 ps, and the oscillator strength is $f_{43} = 0.19$, similar to OWIGS254.

TWIGS254 was MBE grown (wafer number VA0336) and processed similarly to OWIGS271, except that Ta/Au waveguides were employed in place of Ta/Cu, and ridges were defined by dry-etching. Experimental data are shown in Fig. 4. Lasing at $\sim 5.2 \text{ THz}$ is observed up to a heatsink temperature of 25 K. While the lower level parasitic is strongly suppressed, as the shoulder feature at $\sim 11 \text{ V}$ is barely visible, TWIGS254 performed worse than OWIGS254 in terms of operating temperature. For reasons unclear to us (perhaps

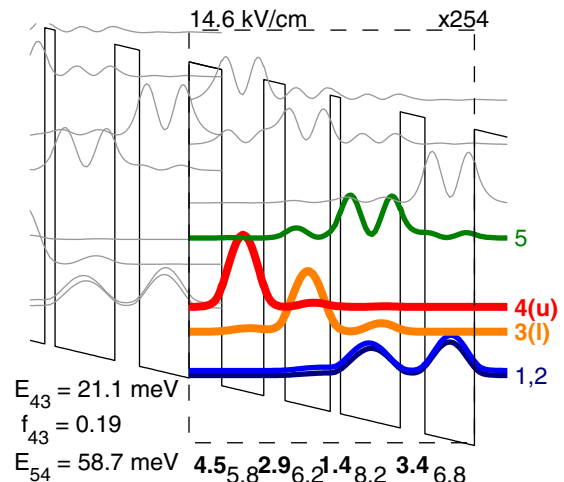


FIG. 3. One module band diagram for TWIGS254. Layers are labeled by their thicknesses in nm. The 3.4 nm barrier is delta-doped in the middle to $2.7 \times 10^{10} \text{ cm}^{-2}$.

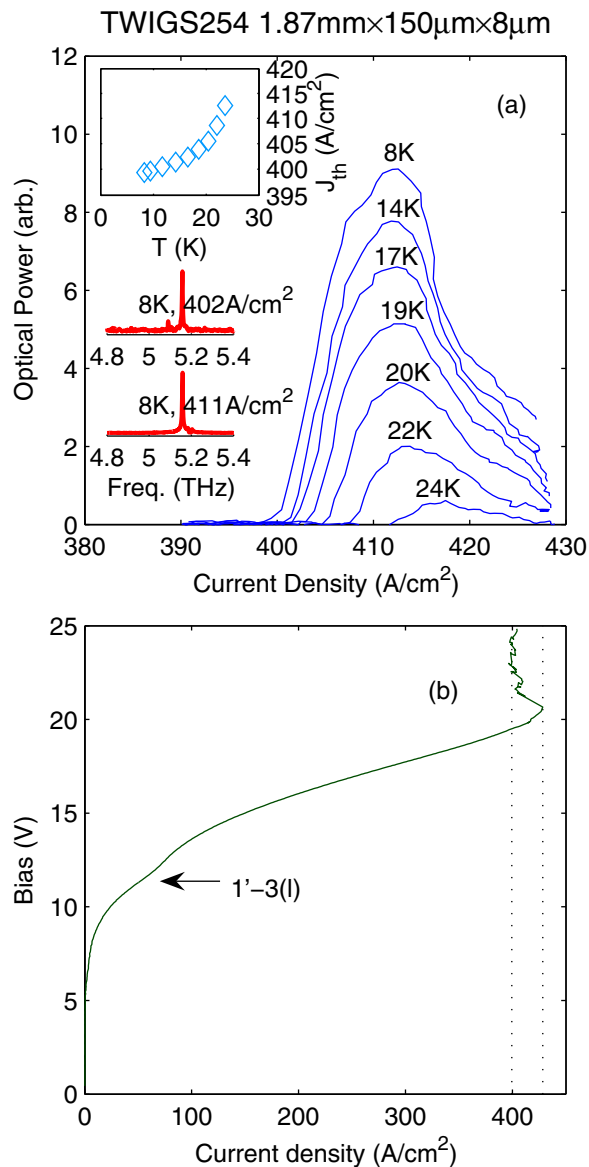


FIG. 4. Experimental data for TWIGS254 clad in Ta/Au waveguides with dry-etched defined mesas. (a) $L-I$ versus temperature. (b) $I-V$ at 8 K. The dotted lines mark the lasing dynamic range in current (compare (a)). The arrow marks the parasitic shoulder attributed to alignment between the injector and lower laser levels.

due to differences in growth and fabrication), the lasing threshold ($\sim 400 \text{ A/cm}^2$) is much higher than that for OWIGS254 ($\sim 310 \text{ A/cm}^2$). Given that both devices have similar maximum current densities ($\sim 420 \text{ A/cm}^2$), the two-well injector device TWIGS254 has a smaller dynamic range and consequently lower T_{max} .

Although lasing action in both designs is achieved, the maximum operating temperatures are rather low. A quick investigation points to an obvious direction for improvement: the lasing threshold current densities are comparable to those of the best RP designs, but the maximum current densities are much lower, yielding a smaller dynamic range. In fact, the difference in dynamic range explains the performance difference between OWIGS271 and TWIGS254. Therefore, an immediate step for improvement is to increase the maximum current densities, which may marginally increase the lasing threshold but should significantly increase the dynamic range.

Another possible cause of overall poor temperature performance in this first try of the GS design is the unusually large radiative gap chosen for both designs ($\sim 20 \text{ meV}$). This choice was motivated by a desire to test the extents of the empirical rule-of-thumb for THz QCLs that $T_{\text{max}} \leq h\nu/k_B$. Kumar *et al.* in Ref. 12 speculate that this result originates from the loss of injection selectivity as the radiative gap shrinks. Conversely, larger radiative gaps are more susceptible to thermally activated LO phonon scattering, which is postulated to be the dominant cause of temperature degradation in THz QCLs. $T_{\text{max}} \leq h\nu/k_B$ has not been previously examined at such high lasing frequencies ($>5 \text{ THz}$), and it is possible that LO phonon scattering induced population inversion degradation overwhelms any benefit to be had from improved injection efficiency.

If this thermally activated LO phonon scattering is the cause of the poor temperature performance, then similar GS designs at lower lasing frequencies will perform better. We can estimate this effect again using rate equations, as mentioned above. For OWIGS271, the estimated low temperature gain assuming a 1 THz gain linewidth is 30 cm^{-1} at $E_{32} = 21.29 \text{ meV}$, and increases to 35 cm^{-1} when $E_{32} = 12 \text{ meV}$. According to gain measurements in Ref. 13, a 5 cm^{-1} improvement in gain could net as much as 50 K improvement in maximum operating temperature, although the crudeness of this estimate must be kept in mind. Alternatively, making the radiative transition even more diagonal ($f < 0.2$) will also increase the upper level lifetime at elevated temperatures.

In conclusion, we report on the experimental realization of THz QCL designs in which no quantum-well excited subbands are involved in transport or lasing. While both lasers performed poorly by present standards, we believe that these results can form the basis for further optimization of this laser architecture. On a lesser note, the demonstration of lasing above 5 THz in both lasers extends the upper limit of frequency coverage by THz QCLs. While low frequency THz QCLs have received much attention in the literature,¹⁴ much less effort has been devoted towards the development of high frequency THz QCLs.

The work at MIT is supported by NASA and NSF. The work at Sandia was performed, in part, at the Center for Integrated Nanotechnologies, a U.S. Department of Energy, Office of Basic Energy Sciences user facility. Sandia National Laboratories is a multiprogram laboratory managed and operated by Sandia Corporation, a wholly owned subsidiary of Lockheed Martin Corporation, for the U.S. Department of Energy's National Nuclear Security Administration under Contract No. DE-AC04-94AL85000.

¹B. S. Williams, *Nature Photon.* **1**, 517 (2007).

²S. Fathololoumi, E. Dupont, C. Chan, Z. Wasilewski, S. Laframboise, D. Ban, A. Mátyás, C. Jirauschek, Q. Hu, and H. C. Liu, *Opt. Express* **20**, 3866 (2012).

³S. Kumar, C. W. I. Chan, Q. Hu, and J. L. Reno, *Appl. Phys. Lett.* **95**, 141110 (2009).

⁴T. Kubis, C. Yeh, P. Vogl, A. Benz, G. Fasching, and C. Deutsch, *Phys. Rev. B* **79**, 195323 (2009).

⁵B. Xu, Ph.D. dissertation, Massachusetts Institute of Technology, Department of Electrical Engineering and Computer Science, 1998.

⁶B. Xu, Q. Hu, and M. R. Melloch, *Appl. Phys. Lett.* **71**, 440 (1997).

- ⁷H. Luo, S. R. Laframboise, Z. R. Wasilewski, G. C. Aers, H. C. Liu, and J. C. Cao, *Appl. Phys. Lett.* **90**, 041112 (2007).
- ⁸S. Kumar, Q. Hu, and J. L. Reno, *Appl. Phys. Lett.* **94**, 131105 (2009).
- ⁹H. Callebaut and Q. Hu, *J. Appl. Phys.* **98**, 104505 (2005).
- ¹⁰E. Dupont, S. Fatholouloumi, Z. R. Wasilewski, G. Aers, S. R. Laframboise, M. Lindskog, S. G. Razavipour, A. Wacker, D. Ban, and H. C. Liu, *J. Appl. Phys.* **111**, 073111 (2012).
- ¹¹C. W. I. Chan, M.S. thesis, Massachusetts Institute of Technology, Department of Electrical Engineering and Computer Science, 2010.
- ¹²S. Kumar, C. W. I. Chan, Q. Hu, and J. L. Reno, *Nat. Phys.* **16**, 166 (2011).
- ¹³D. Burghoff, C. W. I. Chan, Q. Hu, and J. L. Reno, *Appl. Phys. Lett.* **100**, 261111 (2012).
- ¹⁴C. Walther, M. Fischer, G. Scalari, R. Terazzi, N. Hoyler, and J. Faist, *Appl. Phys. Lett.* **91**, 131122 (2007).